

## Space-Charge Driven Emittance Growth in a 3D Mismatched Anisotropic Beam

Ji Qiang and Robert D. Ryne

*Lawrence Berkeley National Laboratory, Berkeley, California 94720, USA*

Ingo Hofmann

*GSI Darmstadt, Planckstrasse 1, 64291 Darmstadt, Germany*

(Received 11 June 2003; published 29 April 2004)

We investigate the phenomenon of space-charge driven emittance growth in a three-dimensional mismatched anisotropic charged particle beam with relevance to high-intensity linear accelerators. The final emittance growth can be understood as a superposition of the contributions from the mismatch-induced halo formation and from the anisotropy-induced energy exchange. The averaged emittance growth per degree of freedom is bounded from above by the so-called “free energy limit” extended by the contributions from energy exchange. The partition of the growth into longitudinal or transverse is, however, a strong function of the tune ratio including the possibility that an initially equipartitioned beam is even driven substantially away from equipartition. The growth of the beam halo extent is dominated by the effect of mismatch, whereas anisotropy itself generates practically no halo.

DOI: 10.1103/PhysRevLett.92.174801

PACS numbers: 41.75.-i, 29.27.Bd

Emittance growth driven by space charge is a fundamental issue in high-intensity linac beam dynamics studies. In recent years a number of studies have been carried out exploring separately the possibility of changing emittances due to beam anisotropy or by mismatch-induced halo formation. Concerning anisotropy alone — in the absence of mismatch — it was found before that the non-linear space-charge forces coupling the longitudinal and transverse directions may cause emittance exchange among different degrees of freedom if some internal resonance conditions are satisfied [1]. The main resonance band in this context is the fourth order difference resonance, which occurs in the vicinity of equal longitudinal and transverse focusing strengths. Note that in a constant focusing channel (smooth approximation of the real machine), the energy anisotropy of the beam is defined in the harmonic oscillator approximation by the ratio  $\epsilon_z k_z / \epsilon_x k_x$ . Here  $z$  is the longitudinal direction and  $x$  is one of the two, basically equivalent, transverse directions;  $\epsilon_z$  and  $\epsilon_x$  are the rms emittances,  $k_z$  and  $k_x$  the focusing wave numbers (i.e., tunes), including space charge in the rms sense, which can be determined from the applied tunes  $k_{z0}$ ,  $k_{x0}$  by means of the rms envelope equations [2,3].

On the other hand, a change of focusing lattice or inadequate knowledge of proper injection conditions can cause a mismatch between the beam and the transport system. The mismatch may result in an oscillation of the beam envelope and generally excite a superposition of the envelope eigenmodes. These envelope modes possess additional free energy compared with the stationary distribution. Particles with appropriate oscillation frequencies can resonate with these envelope modes through the so-called parametric 2:1 resonance and attain large amplitude to form a halo [4,5]. These halo particles extract the energy from the envelope modes and convert the free energy from mismatch into thermal energy, which causes

beam emittance growth. A 2D free-energy model proposed by Reiser [6] for a round beam has recently successfully been applied to the simulation of a 2D coasting beam with equal emittances and arbitrary tune ratios to derive upper bounds for the emittance growth as a function of the mismatch factor [7].

In this paper we consider the simultaneous presence of both effects under a broad range of longitudinal-to-transverse focusing ratios. Simulations are performed by first solving the 3D rms envelope equations to determine the matched rms equilibrium parameters for a beam in a constant focusing channel. Using these parameters, we then generate an initial 6D Gaussian (not truncated) particle distribution. The choice of Gaussian beams is preferable over water bag distribution beams for two reasons: (1) the conversion of mismatch field energy into halo is inhibited for water bag beams due to the lack of initial tails, which provide a seed to the halo [7]; (2) the recent LEDA experiment suggests that linac beams from radio frequency injectors naturally have tails [8]. The simulations have been performed using the 3D particle-in-cell code IMPACT [9], which includes a self-consistent space-charge calculation. We have used  $1 \times 10^6$  particles on a  $64 \times 64 \times 64$  Cartesian grid and free-space boundary conditions. We have used equal transverse focusing strengths ( $k_{x0} = k_{y0}$ ) and equal transverse emittances ( $\epsilon_{x0} = \epsilon_{y0}$ ), so in the 3D simulation the initial distribution in  $y$  is identical to that in  $x$ . When the beam is mismatched, the initial coordinates are scaled by a mismatch factor,  $M$ , in all three directions, and the momenta are scaled by  $1/M$  in all three directions. The particle advance is performed using a second order accurate split-operator method, with 25 steps (i.e., 25 space-charge kicks) within each betatron oscillation period. The constant focusing channel is represented using a linear transfer map between each space-charge kick. The

numerical convergence of the simulation has been checked using a larger number of macroparticles, more grid points, and a smaller step size.

Simulation results are presented below that involve mismatch and equal emittances, no mismatch and unequal emittances, and combined mismatch and unequal emittances. For each case, we present a systematic study of space-charge driven emittance growth as a function of the longitudinal-to-transverse focusing strength ratio,  $k_z/k_x$ . All the simulations have been performed with  $k_x/k_{x0} = 0.6$  and with rms emittance ratios  $\epsilon_z/\epsilon_x = 1$  or  $\epsilon_z/\epsilon_x = 2$ . To perform the parameter scan in  $k_z/k_x$ , we vary both the beam current and the zero current focusing strength ratio while holding  $k_x/k_{x0}$  fixed at 0.6. Finding the matched solution of the 3D rms equations then determines the value of  $k_z/k_x$ .

Before analyzing the results of our parameter studies, we first present in Fig. 1 results from one point in parameter space,  $\epsilon_z/\epsilon_x = 2$ ,  $k_z/k_x = 1.26$ , showing results from two simulations, one with mismatch  $M = 1.3$  and one without mismatch. This example demonstrates the fact that initially anisotropic beams may move *farther away* from isotropy as the beam evolves. In this case, the longitudinal-to-transverse tune ratio is located inside the fourth order resonance band of an rms matched anisotropic beam. We see that without initial mismatch, the emittances from both directions evolve towards each other to approach a more equipartitioned state. With initial mismatch, after a short equipartitioning process, the emittance starts to grow in both directions driven by the mismatch-induced halo formation, but predominately in  $z$ , which leads away from equipartition. The time scales of emittance evolution due to mismatch and anisotropy are approximately the same for the other longitudinal-to-transverse tune ratios within the coupling resonance band. Furthermore, the mismatched emittance growth away from approaching the equipartition does not depend on the special Gaussian initial distribution used in the

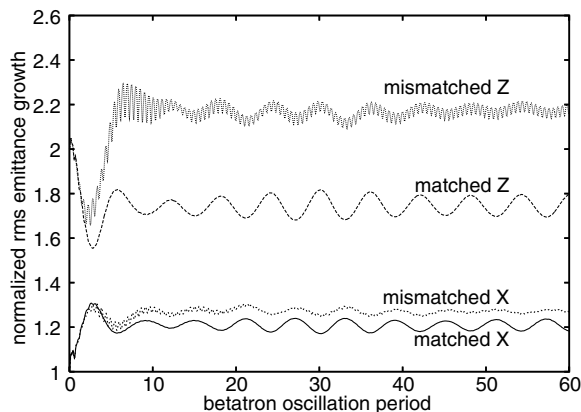


FIG. 1. Evolution of rms emittance for matched and mismatched ( $M = 1.3$ ) initial Gaussian distributions with  $k_{z0}/k_{x0} = 1.025$ ,  $k_x/k_{x0} = 0.6$ ,  $k_z/k_x = 1.26$ , and  $\epsilon_z/\epsilon_x = 2$ .

above figure. A similar growth has also been observed using an initial water bag distribution.

Now we consider the three cases described above.

*Case 1: mismatch and equal emittances ( $M = 1.3$ ,  $\epsilon_z/\epsilon_x = 1$ ).*—Fig. 2 shows the final relative rms emittance growth as a function of  $k_z/k_x$ . The simulations were done through 100 zero current betatron oscillation periods to reach saturated amplitudes. In this case the emittance exchange around the fourth order difference resonance  $2k_z - 2k_x \approx 0$  is negligible since there is no free energy available to transfer for a beam with equipartitioned temperature ratio  $T_z/T_x = 1$ . For  $0.56 < k_z/k_x < 1$ , the relative emittance growth in the transverse direction is larger than that in the longitudinal direction. Above  $k_z/k_x = 1$ , the emittance growth in the longitudinal direction becomes dominant. In both cases, the emittance growth is predominately in the direction with stronger focusing. Such anisotropic emittance growth could make the beam move farther away from equipartition. It has been shown by Franchetti *et al.* that around  $k_z/k_x = 1$ , with stronger focusing in a given plane, the fixed point in that plane for the typical 2:1 parametric resonance moves closer to the core [7]. This results in more particles being involved in the parametric resonance in that plane and larger emittance growth. Greater final emittance growth in the longitudinal direction is observed for  $k_z/k_x < 0.56$ . The large final longitudinal emittance growth is associated with the contributions from the halo formation and from the equipartitioning driven by a higher order mode instability [10].

*Case 2: no mismatch and unequal emittances ( $M = 1$ ,  $\epsilon_z/\epsilon_x = 2$ ).*—In this case (Fig. 3), the presence of a major fourth order coupling resonance within the resonance band  $2k_z - 2k_x \approx 0$  leads to pronounced emittance exchange between the transverse direction and the longitudinal direction even though the beam is initially rms matched. It should be noted that the usual fourth order

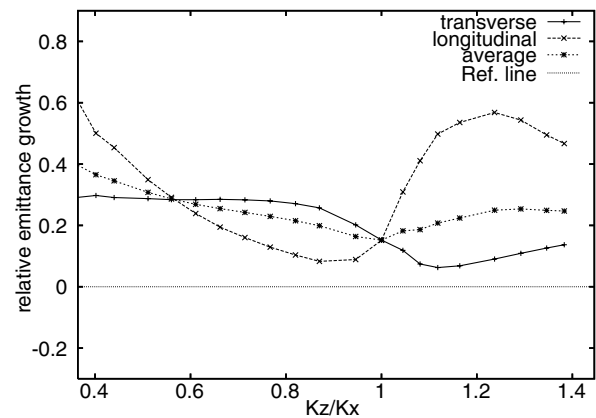


FIG. 2. Final relative rms emittance growth in the longitudinal direction, transverse direction, and averaged per degree of freedom as a function of the tune ratio  $k_z/k_x$  ( $k_x/k_{x0} = 0.6$ ,  $\epsilon_z/\epsilon_x = 1$ ) for an initial mismatched ( $M = 1.3$ ) Gaussian distribution.

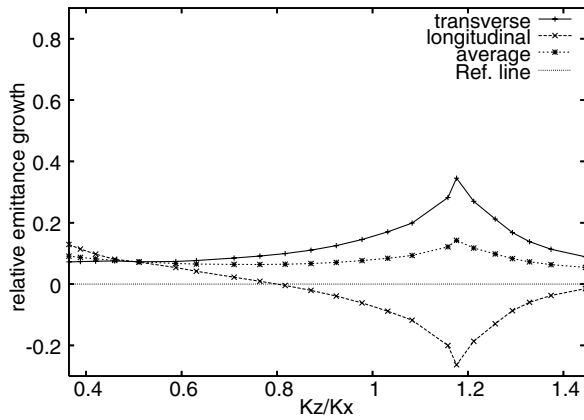


FIG. 3. Final relative rms emittance growth in the longitudinal direction, transverse direction, and averaged per degree of freedom as a function of the tune ratio  $k_z/k_x$  ( $k_x/k_{x0} = 0.6$ ,  $\epsilon_z/\epsilon_x = 2$ ) for an initial matched Gaussian distribution.

coupling resonance condition  $2k_z - 2k_x = 0$  applies only to the limit of vanishing space-charge forces. Because of the space-charge forces, there is a coherent response of charge distribution which leads to a shift of the resonance condition [11]. In this case the peak of the emittance exchange is around  $k_z/k_x = 1.18$  instead of 1. As seen in the figure, within the resonance band  $2k_z - 2k_x \approx 0$ , the maximum longitudinal emittance decreases by about 26%, while the maximum transverse emittance increases by about 34%. The energy anisotropy  $T_z/T_x$  has dropped from an initial 2.3 to 1.1 at the peak of resonance. The emittance growth averaged per degree of freedom is not sensitive to the variation of the tune ratio except near the peak of the coupling resonance, where about 10% is observed.

*Case 3: Combined mismatch and unequal emittances* ( $M = 1.3$ ,  $\epsilon_z/\epsilon_x = 2$ ).—Fig. 4 shows that, with the presence of initial mismatch in the above anisotropic beam, the final emittance growth within the fourth order reso-

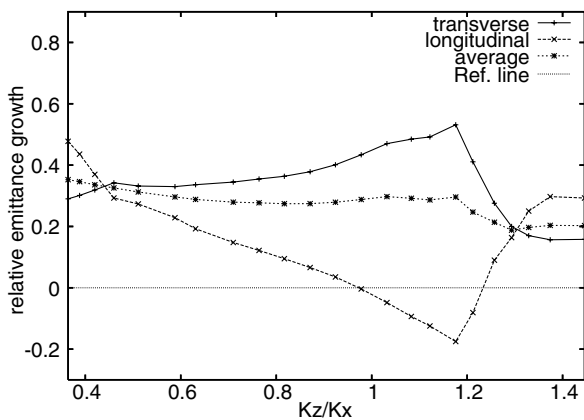


FIG. 4. Final relative rms emittance growth in the longitudinal direction, transverse direction, and averaged per degree of freedom as a function of the tune ratio  $k_z/k_x$  ( $k_x/k_{x0} = 0.6$ ,  $\epsilon_z/\epsilon_x = 2$ , and  $M = 1.3$ ) for an initial Gaussian distribution.

nance band  $2k_z - 2k_x \approx 0$  for the rms matched beam is significantly modified. The mismatch causes envelope oscillations and halo formation in both the transverse and longitudinal directions. As a result, the emittances grow in both directions even with the presence of initial emittance exchange. Comparing the matched anisotropic beam with  $\epsilon_z/\epsilon_x = 2$ , the peak of the resonant emittance exchange occurs at the same tune ratio. However, the range of tune ratio for the final emittance exchange has been reduced from  $0.8 < k_z/k_x < 1.45$  to  $0.97 < k_z/k_x < 1.24$ . Within this range, the fourth order resonance driven equipartitioning is stronger than the halo driven emittance growth. There is a net final emittance exchange between the longitudinal direction and the transverse direction. Outside this range, the opposite is true. The emittance growth from the mismatched halo overcomes the initial equipartitioning process. The final state of the beam can be driven farther away from equipartition.

An important finding is that, for all these cases, the averaged rms emittance growth per degree of freedom is found to be relatively insensitive to the ratio of the tune within the range  $0.6 < k_z/k_x < 1.4$ . (This holds despite the fact that there is strong dependence on the tune ratio in the transverse and the longitudinal directions separately.) This makes it feasible to estimate the average emittance growth and to compare with the “free-energy” limit derived by Reiser for a symmetrically focused coasting beam [2]. The latter is a 2D approximation understood as the maximum possible rms emittance growth, if all of the energy added to an axially symmetric beam by radial mismatch is “decohered” and a new matched uniform beam is obtained—regardless of the actual driving mechanism. Figure 5 shows the averaged rms emittance growth as a function of the mismatch factor for an initial Gaussian beam with  $k_{z0}/k_{x0} = 1$ ,  $\epsilon_z/\epsilon_x = 1$  and 2 together with the emittance growth calculated from the free-energy model. The emittance growth using the 2D free-energy model includes the contribution from the

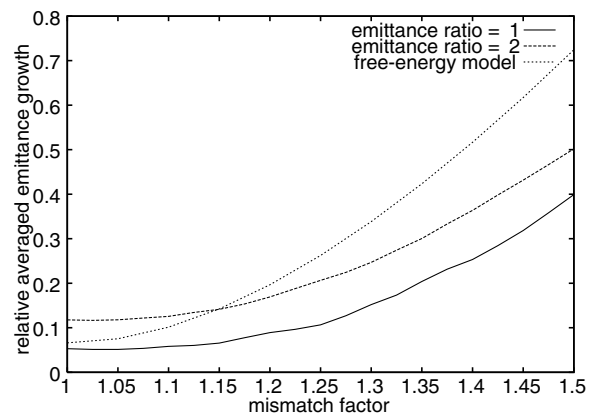


FIG. 5. Relative averaged rms emittance growth with  $\epsilon_z/\epsilon_x = 1$ ,  $\epsilon_z/\epsilon_x = 2$ , and compared with the free-energy theory, as a function of the mismatch factor for Gaussian beams ( $k_x/k_{x0} = 0.6$ ,  $k_{z0}/k_{x0} = 1.0$ ).

charge redistribution of a initial Gaussian beam to a final uniform distribution and the contribution from the initial envelope mismatch to a uniform beam. This free-energy model overestimates the emittance growth in a real system since the final distribution is usually not a uniform distribution. Hence, the free energy released from the initial mismatched beam is less than that used in the 2D free-energy model. Besides the additional offset for  $M = 1$  due to equipartition, the averaged emittance growth per degree of freedom for  $\epsilon_z/\epsilon_x = 1$  and  $\epsilon_z/\epsilon_x = 2$  rises quite similarly. Without the initial offset, the emittance growth from the simulations is visibly less than that predicted by the free-energy model. The smaller averaged emittance growth from simulations is due to the fact that there is an incomplete transfer of free energy of the envelope oscillation to the emittance growth. However, for an anisotropic beam, the 2D free-energy model has to be corrected with the contributions from the energy anisotropy in order to represent an upper bound for the averaged emittance growth per degree of freedom.

For a mismatched anisotropic beam, the halo extent beyond rms can be quantified by the ratio of  $\epsilon_{99.99\%}/\epsilon_{\text{rms}}$  (initially  $\approx 18$  for a Gaussian). Here,  $\epsilon_{99.99\%}$  is defined from the ellipse with an area containing 99.99% particles of the beam [12]. Figure 6 shows the normalized final 99.99% emittance, averaged over  $x$  and  $z$ , as a function of the tune ratio  $k_z/k_x$  with/without an initial mismatch. The halo extent, as determined from the square root of the 99.99% emittance, is seen to be relatively insensitive to the tune ratio and exceeds  $9\sigma$  in radius for  $k_z/k_x < 1.2$ . It is also seen that the averaged 99.99% emittance growth in an initial mismatched anisotropic beam is about 2 to 3 times of the matched anisotropic beam. This suggests that the extent of the beam is dominated by the mismatched halo formation instead of the energy anisotropy. The rms emittance growth driven by the energy anisotropy occurs in the core of the beam and has little effect on the beam halo.

In summary, we have found that outside the space-charge coupling resonance band, emittance growth is dominated by the rms mismatched halo formation. Within the resonance band, the final emittance growth shows a superposition of the contributions from the energy exchange and from the mismatched halo formation. In this region the beam can be pushed farther away from equipartition by the mismatch-induced emittance growth. Even though the emittance growth along the transverse and longitudinal directions shows a strong dependence on the longitudinal-to-transverse tune ratio, the averaged rms emittance growth per degree of freedom is relatively insensitive to the tune ratio. Furthermore we have found that, in our 3D studies, the averaged growth per degree of freedom follows the bound of the 2D free-energy model of Reiser plus the contributions from an-

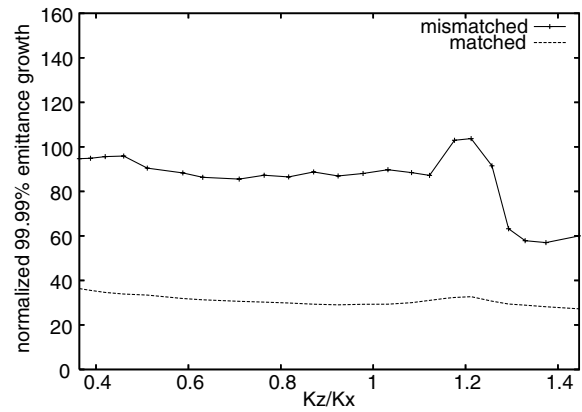


FIG. 6. Final 99.99% emittance relative to the initial rms emittances for the initial Gaussian distribution of Figs. 3 and 4.

isotropic energy exchange. While the rms emittance growth depends on both the energy anisotropy and the envelope mismatch, the growth of the beam halo extent which is quantified by the ratio of  $\epsilon_{99.99\%}/\epsilon_{\text{rms}}$  is clearly controlled by the mismatch-induced halo formation.

The author (J. Q.) would like to thank Dr. R. Kishek, Dr. N. Pichoff, and Dr. H. Qin for discussions. This research used resources of the National Energy Research Scientific Computing Center. This work was performed under the auspices of a Scientific Discovery through Advanced Computing project, “Advanced Computing for 21st Century Accelerator Science and Technology,” which is supported by the U.S. DOE/SC Office of High Energy Physics and the Office of Advanced Scientific Computing.

- 
- [1] I. Hofmann, J. Qiang, and R. Ryne, *Phys. Rev. Lett.* **86**, 2313 (2001).
  - [2] M. Reiser, *Theory and Design of Charged Particle Beams* (John Wiley & Sons, New York, 1994).
  - [3] R. D. Ryne, *acc-phys/9502001*.
  - [4] R. L. Gluckstern, *Phys. Rev. Lett.* **73**, 1247 (1994).
  - [5] T. P. Wangler, K. R. Crandall, R. Ryne, and T. S. Wang, *Phys. Rev. ST Accel. Beams* **1**, 084201 (1998).
  - [6] M. Reiser and N. Brown, *Phys. Rev. Lett.* **74**, 1111 (1995).
  - [7] G. Franchetti, I. Hofmann, and D. Jeon, *Phys. Rev. Lett.* **88**, 254802 (2002).
  - [8] C. K. Allen *et al.*, *Phys. Rev. Lett.* **89**, 214802 (2002).
  - [9] J. Qiang, R. Ryne, S. Habib, and V. Decyk, *J. Comput. Phys.* **163**, 434 (2000).
  - [10] I. Hofmann, *Phys. Rev. E* **57**, 4713 (1998).
  - [11] I. Hofmann, G. Franchetti, O. Boine-Frankenheim, J. Qiang, and R. Ryne, *Phys. Rev. ST Accel. Beams* **6**, 024202 (2003).
  - [12] T. P. Wangler, *Principles of RF Linear Accelerators* (John Wiley & Sons, New York, 1998).